bioRxiv preprint doi: https://doi.org/10.1101/2024.08.05.606726; this version posted August 6, 2024. The copyright holder for this preprint (which was not certified by peer review) is the author/funder. All rights reserved. No reuse allowed without permission.

DNA spontaneously wrapping around a histone core prefers negative supercoiling: A Brownian dynamics study

Chunhong Long[1†], Hongqiong Liang[1‡] Biao Wan[2*],

1 School of Science, Chongqing University of Posts and Telecommunications, Chongqing, China
2 Wenzhou Institute, University of Chinese Academy of Sciences, Wenzhou, China

†longch@cqupt.edu.cn
‡2406883795@qq.com
* wanbiao@ucas.ac.cn

Abstract

In eukaryotes, DNA achieves a highly compact structure primarily due to its winding around the histone cores. The nature wrapping of DNA around histone core form a 1.7 left-handed superhelical turns, contributing to negative supercoiling in chromatin. On the contrary, negative supercoils generated behind the polymerase during transcription may play a role in triggering nucleosome reassembly. To elucidate how supercoils influence the dynamics of wrapping of DNA around the histone cores, we developed a novel model to simulate the intricate interplay between DNA and histone. Our simulations revealed that both positively and negatively supercoiled DNAs are capable of wrapping around histone cores to adopt the nucleosome conformation. Most of all, our findings confirmed a preference for negative supercoiled DNA during nucleosome wrapping, and revealed that the both of the negative writhe and twist are comparatively beneficial to the formation of the DNA wrapping around histone. This advancement in the understanding of spontaneously nucleosome formation may provide insights into the intricate dynamics of chromatin assembly and its diverse functions. Our model thus can be further utilized to simulate the formations of multi-nucleosomes during re-assembling of the chromatin fiber, which will significantly enhance the understanding of the fundamental mechanisms governing the structure and function of chromatin.

Author summary

The compacted organization of DNA within chromatin is primarily attributed to its intricate winding around histone cores. This winding process involves 1.7 left-handed superhelical turns around the histone core, contributing to the negative supercoiling within chromatin fibers. To gain deeper insights into how DNA supercoiling impacts the dynamics of DNA wrapping around histone cores, we devised a novel computational model that simulates the intricate interplay between DNA and histone cores. Additionally, our simulations revealed that both of the positively and negatively supercoiled DNA can spontaneously adopt the nucleosome conformation upon wrapping around the histone core, and demonstrated a preferential tendency for negative supercoiling during nucleosome wrapping. Finally, we examined that both the negative writhe and twist components are comparatively advantageous for the formation of the nucleosome. The studies shed light on the intricate dynamics underlying chromatin assembly and its functional implications.

bioRxiv preprint doi: https://doi.org/10.1101/2024.08.05.606726; this version posted August 6, 2024. The copyright holder for this preprint (which was not certified by peer review) is the author/funder. All rights reserved. No reuse allowed without permission.

Introduction

In eukaryotes, the primary step in the intricate folding of DNA into chromatin involves the wrapping of DNA strands around the histone core [1]. The crystal structure of the histone core particle of chromatin contains two copies of each histone protein, H2A, H2B, H3 and H4 being assembled into an octamer that accommodates approximately about 145 base pairs (bp) wrapped around it [2–5]. The negatively charged DNA wraps around the positively charged histone proteins about two turns in a counter-clockwise fashion [6, 7].The left-handed wrapping of DNA around the histone octamer results in the formation of approximately 1.7 superhelical turns [1, 8]. The packaging of DNA within a robust nucleosome framework in eukaryotes physically obstructs the establishment of the initial replication and transcription complexes, as well as the subsequent activities of the respective machineries. Conversely, during transcription elongation, the positive supercoils generated in front of the RNA polymerase may destabilize the nucleosome while the negative supercoils behind the polymerase may aid in triggering the nucleosome reassembling [9, 10]. Recent biochemical and molecular biological experiments have focused on stretching DNA molecules to investigate their mechanical or dynamical behaviors [6, 11–14]. Meanwhile, some theoretical works have also explored the mechanical or dynamical properties of DNA and chromatin [15–17]. Along with experimental and theoretical studies of DNA and chromatin, numerous molecular dynamics simulation studies had been done on structures and stabilities of nucleosomes [18–25]. Recently, the Brownian dynamics methods had been developed, which have been employed to study the kinetics of DNA and nucleosome interactions, providing further insights into the dynamic nature of chromatin assembly and function [15, 26–32].

In this study, we developed a Brownian dynamics model to investigate the dynamics properties of spontaneously nucleosome wrapping by supercoiled DNA. Our model integrated a discrete worm-like chain and a rotational sphere, for representing DNA and histone, respectively. Employing this model, we confirmed that the interaction between histone and DNA is the primary driving force behind nucleosome wrapping, regardless of the supercoiling density of the DNA. Furthermore, our simulations demonstrated that negative supercoils are more beneficial to spontaneous nucleosome wrapping, which supports that negative supercoils facilitate the wrapping of DNA around histone octamers, thereby promoting the formation of nucleosomes. And finally we discussed the mechanisms underlying the preference for negative supercoiling during nucleosome wrapping. Our findings provide insights into how the DNA supercoiling impacts chromatin structure, function and assembly.

Method

Our coarse grained model consists of a discrete worm-like chain and a rotational sphere, depicted in FIG 1, to simulate the supercoiled DNA and the histone core, respectively.

The discrete worm-like chain is comprised of N jointed discrete segments (cylinders) [33]. The conformation of this chain is described by $N+1$ vertices $\{\mathbf{r}_i\}$. The i-th segment is defined by the vector $\mathbf{s}_i \equiv \mathbf{r}_{i+1} - \mathbf{r}_i$. The equilibrium length of each segment is $l_0 = 3.4nm$, representing 10 bp. In addition, an orthogonal base vector frame $\{\mathbf{e}_i, \mathbf{f}_i, \mathbf{g}_i\}$ ($\mathbf{e}_i = \mathbf{f}_i \times \mathbf{g}_i$) is attached to the segment (Fig 1), where $\mathbf{e_i} \equiv \mathbf{s_i}/s_i$, $\mathbf{f}_i$ and $\mathbf{g}_i$ describe a local rotational angle φ_i of the segment about its axis $\mathbf{e}_i$. The torsion of the chain is described by N rotational angles $\{\varphi_i\}$. The i-th bending angle β_i is defined as $\arccos(\mathbf{e}_{i-1} \cdot \mathbf{e}_i)$. The i-th twist θ_i depends on the two frames $\{\mathbf{f}_{i-1}, \mathbf{g}_{i-1}, \mathbf{e}_{i-1}\}$ and $\{\mathbf{f}_i, \mathbf{g}_i, \mathbf{e}_i\}$. By introducing an auxiliary vector $\mathbf{p_i} = \mathbf{e_{i-1}} \times \mathbf{e_i}$, the twist is $\theta_i = \alpha_i + \gamma_i$, where α_i is the rotation angle from $\mathbf{f}_{i-1}$ towards $\mathbf{p_i}$, γ_i is the angle from $\mathbf{p_i}$ towards $\mathbf{f}_i$.

bioRxiv preprint doi: https://doi.org/10.1101/2024.08.05.606726; this version posted August 6, 2024. The copyright holder for this preprint (which was not certified by peer review) is the author/funder. All rights reserved. No reuse allowed without permission.

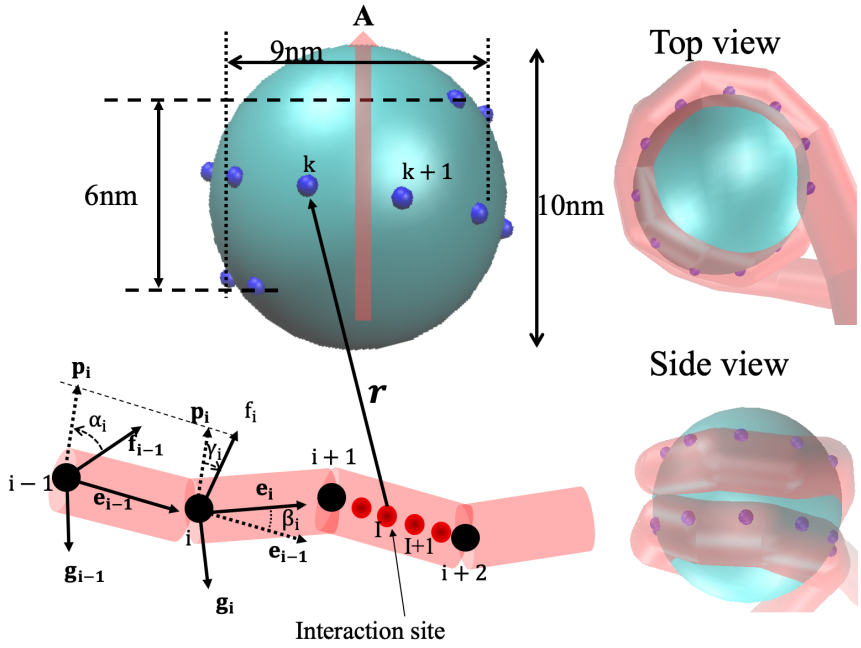


Fig 1. Schematic view of the histone core and DNA interaction model. The histone core is modeled as a sphere entity, possessing 20 interaction points along a left-handed helical path that enable the DNA to be wound around the histone core. The axial vector $\mathbf{A}$ of the helical path on the sphere describes the orientation of the histone core. The DNA is modeled as N discrete segements. The i-th segment is defined by vertices i and $i+1$, attached by $\mathbf{f}_i$, $\mathbf{g}_i$ and $\mathbf{e}_i$. The vectors define the bending angle $\beta_i = \arccos(\mathbf{e}_{i-1} \cdot \mathbf{e}_i)$, and the twisting angle $\theta_i = \alpha_i + \gamma_i$ by introducing an auxiliary vector $\mathbf{p_i} = \mathbf{e_{i-1}} \times \mathbf{e_i}$. (Right) Two views of the nucleosome structure generated by VMD from the simulations.

bioRxiv preprint doi: https://doi.org/10.1101/2024.08.05.606726; this version posted August 6, 2024. The copyright holder for this preprint (which was not certified by peer review) is the author/funder. All rights reserved. No reuse allowed without permission.

The stretching, bending, twisting potential energies are all harmonic [33]. The electrostatic interaction is represented as the Debye-Hückel potential on the uniformly distributed point-like charges on the segments [34–36]. Thus the energetics of the DNA chain is

$$E = \sum_{i=0}^{N-1} \frac{k_B T}{2(l_0 \alpha_s)^2}(l_0 - s_i)^2 + \sum_{i=1}^{N-1} k_B T \alpha_b \beta_i^2 + \sum_{i=1}^{N-1} \frac{\alpha_t}{2l_0}\theta_i^2 + \frac{\nu^2 l_0^2}{\lambda^2 D_e} \sum_{I=0}^{\lambda N} \sum_{J=I+N_{near}+1}^{\lambda N} \frac{exp(-\kappa r_{IJ})}{r_{IJ}}, \tag{1}$$

where the first term on the right-hand side is the stretching energy of each segment and α_s is a stiffness coefficient; the second term is the bending energy and α_b is a bending stiffness coefficient; the third one is the twisting energy and α_t is a torsional stiffness coefficient [33]; the last one is the electrostatics and ν and λ are the effective charge density on each segment and the number of the point-like charges per segment, respectively, D_e is the dielectric constant of water, N_{near} is the number of neighbor point-like charges of each segment, and κ is the inverse Debye length. Moreover, the impenetrability of DNA segments is guaranteed by introducing a repulsion force $\mathbf{F}_{IJ}^{ex} = -F_{ex}\frac{\mathbf{r}_{IJ}}{r_{IJ}}$ if $r_{I,J} < 2nm$ [34], where the indices I and J denote the point-like charges, not the vertices. All the simulation parameters used in this method are listed in the TABLE 1.

The histone core is considered as a rotational sphere with diameter $10nm$, on which 20 discrete interaction points are distributed along a left-handed helical path, spanning approximately 1.7 turns. The helical path of these interaction sites extends vertically for a height of 6 nm, while the diameters of the helix's apical and basal termini approximate 9 nm.

The interactions between the DNA and the points on the sphere are modeled as the Morse potential [29]

$$U_{DH} = \sum_{k,I} \epsilon \left[(e^{-\alpha(r-\delta)} - 1)^2 - 1 \right] \tag{2}$$

where ϵ is the absorption energy, appropriately chosen as $5k_BT$ (corresponding to the absorption energy density $8k_BTnm^{-1}$) [29, 30], $\alpha \sim 1.26nm$, is the inverse decay length, $\delta = 1nm$, specifies the radius of the repulsive core of DNA, r is the distance between the I-th DNA binding site and the k-th site on the histone. The excluded volume effect between DNA and histone is considered by a half-harmonic potential, i.e., for $r < |a| + r_0$,

$$U_{ex} = \frac{1}{2}k(|a| + r_0 - R)^2 \tag{3}$$

where $k = 2k_BT$ is the rigidity coefficient, $|a| = 5nm$ is the radius of the histone, $r_0 = 1nm$ is the radius of DNA and R is the distance between the I-th DNA binding site and the center of the histone.

The Brownian dynamics (BD) can be performed using an integration, the second-order BD algorithm [33, 35]. A tentative first-order displacement is

$$\begin{aligned} \mathbf{r'}_i(t+\Delta t) - \mathbf{r}_i(t) &= \sum D_{ij}(t)\frac{\mathbf{F}_j(t)}{k_BT}\Delta t + \mathbf{R}_i \\ \varphi'_i(t+\Delta t) - \varphi_i(t) &= D_{rot}(t)\frac{T_i^t(t)}{k_BT}\Delta t + \Phi_i \end{aligned}, \tag{4}$$

and the final half-step is

$$\begin{aligned} \mathbf{r}_i(t+\Delta t) - \mathbf{r}'_i(t+\Delta t) &= \sum D_{ij}(t)\frac{-\mathbf{F}_j(t) + \mathbf{F}'_j(t+\Delta t)}{2k_BT}\Delta t \\ \varphi_i(t+\Delta t) - \varphi'_i(t+\Delta t) &= D_{rot}(t)\frac{-T_{q,i}(t) + T'_{q,i}(t+\Delta t)}{2k_BT}\Delta t \end{aligned}, \tag{5}$$

bioRxiv preprint doi: https://doi.org/10.1101/2024.08.05.606726; this version posted August 6, 2024. The copyright holder for this preprint (which was not certified by peer review) is the author/funder. All rights reserved. No reuse allowed without permission.

Table 1. Constants and parameters

Parameter	Symbol	Value [33, 35]
Number of segments	N	100
Temperature	T	$298K$
Histone core radius	R_h	$5nm$
Segment equilibrium length	l_0	$3.4nm$
Stretching stiffness coefficient	α_s	0.1
Bending stiffness coefficient	α_b	7.32
Torsional stiffness coefficient	α_t	$400pN \cdot nm^2$
Monovalent salt concentration		150 mM
Dielectric constant	D_e	$8.9 \times 10^{-9} F/m$
Effective charge density	ρ_e	$8.01e/nm$
Inverse Debye length	κ	$1.261nm^{-1}$
Number of the point charges per segment	λ	5
Electrostatic cutoff distance	r_c	$8nm$
DNA excluded volume force	F_{ex}	$15pN$
Viscosity	η	$0.001kg/(m \cdot s)$
Hydrodynamic DNA radius	R_H	$1.3nm$
Hydrodynamic DNA rotational radius	R_d	$1.2nm$
Simulation time-step size	Δt	$25ps$

where $\mathbf{r}'_i$ is the tentative position, D_{ij} is the Rotne-Prager tensor component [33], and for the computational efficiency, we chose $D_{ij} = D\delta_{ij} = \delta_{ij} k_B T / 6\pi\eta R_H$, and here R_H is effective radius of each segment [35, 37], $\mathbf{F}_i$ and $\mathbf{F}'_i$ are the forces on the i-th vertex corresponding to the conformation $\mathbf{r}$ and $\mathbf{r}'$, respectively, $T_{q,i}$ and $T'_{q,i}$ are the torques on the i-th segment; $D_{rot} = k_B T / 4\pi\eta R_d^2 l_0$ is the rotational diffusion constant, here R_d is the diffusion radius of DNA, $\mathbf{R}$ and Φ are the thermal noises with the properties $\langle \mathbf{R} \rangle = 0$, $\langle \mathbf{R} \otimes \mathbf{R} \rangle = 2\mathbf{D}\Delta t$, $\langle \mathbf{\Phi} \rangle = 0$, $\langle \mathbf{\Phi} \otimes \mathbf{\Phi} \rangle = 2\mathbf{D_{rot}}\Delta t$.

The center of mass of the histone protein moves following the Langevin equation under the protein-DNA interactions $U_{DH} + U_{ex}$,

$$\dot{\mathbf{R}}_{COM} = -\frac{1}{\zeta} \nabla_{R_{COM}} (U_{DH} + U_{ex}) + \sqrt{\frac{2k_B T}{\zeta}} \mathbf{w} \tag{6}$$

where $\zeta = 6\pi\eta|a|$ is the the friction coefficient, with η the solution viscosity and $|a|$ the radius of the spherical protein, and $w(t)$ is the Gaussian noise with zero mean and unit variance. It should be noted that the BD (EQ.6) can be performed using the second-order BD algorithm.

The orientational or rotational degrees of the histone core caused by thermal fluctuations and interactions are modeled by partitioning the rotations into the spatial rotation of the unit axial vector $\mathbf{A}$ (axial vector of the helical path), $\mathbf{\Delta\Omega}_A$ and the spinning about $\mathbf{A}$, Ψ [38]. Accordingly, the protein angular Langevin dynamic equations are formulated as (details in Text S1).

$$\mathbf{A} \times \dot{\mathbf{\Omega}}_A |\mathbf{a}| = -\frac{1}{\zeta_{rot}} \sum_i (\mathbf{a} \times \mathbf{F}_i) \times \mathbf{A}/|\mathbf{a}| + \sqrt{\frac{2k_B T}{\zeta_{rot}}} (\mathbf{A} \times \mathbf{e}_\Theta w_1 + \mathbf{A} \times \mathbf{e}_\Phi w_2) \tag{7}$$

$$\mathbf{A} \cdot \dot{\mathbf{\Psi}} |\mathbf{a}| = -\frac{1}{\zeta_{rot}} \sum_i (\mathbf{a} \times \mathbf{F}_i) \cdot \mathbf{A}/|\mathbf{a}| + \sqrt{\frac{2k_B T}{\zeta_{rot}}} (w_3) \tag{8}$$

bioRxiv preprint doi: https://doi.org/10.1101/2024.08.05.606726; this version posted August 6, 2024. The copyright holder for this preprint (which was not certified by peer review) is the author/funder. All rights reserved. No reuse allowed without permission.

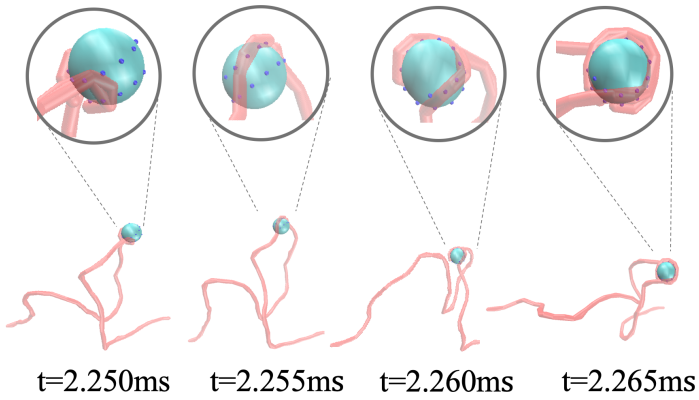


Fig 2. Representative conformations of DNA winding around a histone core obtained from the Brownian dynamics simulations. A single histone core interacts with a positively supercoiled DNA ($\sigma = 0.03$) at length of 1000 bp (100 segments) under tension $f = 0.1pN$.

where $\zeta_{rot} = 8\pi\eta|a|$ is the friction due to rotation of the protein in solution, w_1,w_2 and w_3 are the Gaussian noises with zero mean and unit variance. The source code is available at: `https://figshare.com/s/b38438c966505126910e`.

Results

Spontaneously wrapping of DNA around histone

A relaxed B-DNA consisting of N base pairs has a linking number $Lk_0 = N/10.5$. The excess linking number difference of a supercoiled DNA is then $\Delta Lk \equiv Lk - Lk_0$. The supercoil density is accordingly defined as $\sigma = \frac{\Delta Lk}{Lk_0}$. When a histone is completely wrapped by DNA, which contributes to approximately -1 linking number difference.

In FIG.2, an extended and supercoiled DNA ($\Delta Lk = 3, i.e., \sigma = \frac{\Delta Lk}{Lk_0} = 0.03$) at length $1000bp$ stretched by $f = 1.0pN$ interacts with a histone. The interactions between DNA and histone with absorption energy $\epsilon = 5k_BT$ can wind the DNA around the histone core, forming a partially wrapped structure, and finally trigger the completion of the nucleosome wrapping.

It should be noted that the nucleosome state induces an extra $\Delta\Delta Lk = +1$ to the unconstrained DNA, which is energetically adverse. However, our simulation suggests that the positive supercoil is able to wrap a histone to form nucleosome.

Strong interaction between histone and DNA promotes the nucleosome wrapping

The DNA winding around the histone core is energetically costly. Hence, the interactions between the DNA and histone should be the primary factor for nucleosome wrapping. The conformations exhibited by the histone-DNA complex can be broadly categorized into three types: mis-wrapped (non-left-handed), partially wrapped and nucleosome wrapped states(FIG.3(a)). The typical pathways of the nucleosome wrapping are *mis-wrapped state→partially wrapped state→nucleosome state* and *partially wrapped state→nucleosome state* (see the Text S2 for the details).

Intuitively, the strong interactions can promote the completion of the nucleosome wrapping. This is confirmed by our simulations of spontaneously nucleosome-wrapping

bioRxiv preprint doi: https://doi.org/10.1101/2024.08.05.606726; this version posted August 6, 2024. The copyright holder for this preprint (which was not certified by peer review) is the author/funder. All rights reserved. No reuse allowed without permission.

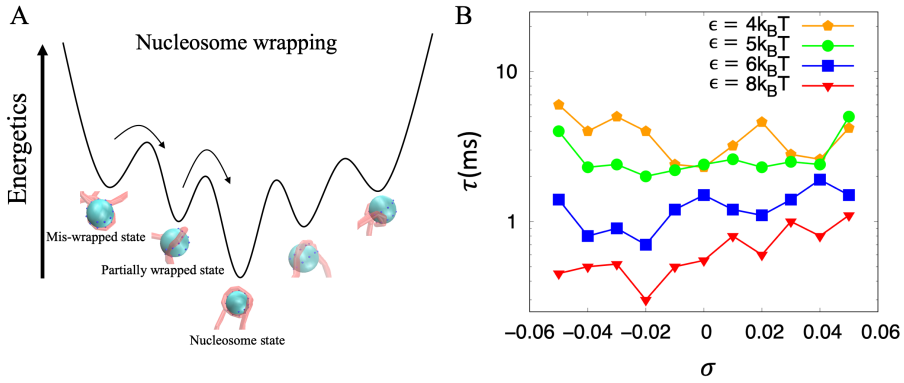


Fig 3. (A) Schematic illustration of the nucleosome wrapping process. Before completely nucleosome wrapping (Energetic minimum), the system explores a vast number of conformations of the mis-wrapped state (out of left-hand helix path) and partially wrapped state. (B) The mean first passage time (MFPT) for the completion of the nucleosome wrapping depends on the interaction energy strength ϵ and the supercoil density σ. Each dot was obtained from 20 simulations trajectories with $10ms$ of each. For each given linking number, the DNA is stretched under constant force $f = 0.3pN$.

with different DNA supercoil densities $-0.05 \leq \sigma \leq 0.05$ and different adsorption energy strength ϵ ($4k_BT, 5k_BT, 6k_BT$ and $8k_BT$, corresponding to the absorption energy density from $6k_BTnm^{-1}$ to $11k_BTnm^{-1}$) under stretching force $f = 0.3pN$ (FIG 3(b)). The interactions from weak to strong correspond to the salt concentrations from high to low. For appropriate absorption energy strengths ($\epsilon = 4k_BT$ and $5k_BT$, corresponding to absorption energy density from $6k_BTnm^{-1}$ to $8k_BTnm^{-1}$), the mean first passage time (MFPT) of nucleosome-wrapping is insensitive to the DNA supercoil density. Notably, under conditions of strong absorption ($\epsilon \geq 6k_BT$), the presence of negative supercoils serves to augment the efficiency of nucleosome wrapping.

Nucleosome-wrapping prefers negative supercoils

During transcription, the positive supercoils generated by the polymerases could dissociate the nucleosomes, while the negative supercoils behind might facilitate the re-assembly of the nucleosomes [9, 10]. Nevertheless, we have demonstrated that the nucleosome-wrapping process shows no sensitivity to the DNA supercoil density for the DNA-histone complex with an appropriate absorption energy strength under a small force (FIG.3b). The efficiency of nucleosome-wrapping is supposed to be force-dependent. Hence, we have compared the mean first passage time (MFPT) of nucleosome wrapping for supercoiled DNAs under different forces. (FIG 4(b)).

In the case of small applied force $f = 0.1pN$, the nucleosome-wrapping efficiency is insensitive to supercoil density. However, for tensional DNA, e.g, $f \geq 0.5pN$, the MFPT for nucleosome wrapping by negative supercoiled DNA is significantly shorter compared to that achieved by positively supercoiled DNA. Notably, for the case of $f = 1.0pN$, the efficiency of nucleosome wrapping under negative supercoils is over an order of magnitude higher than that under positive supercoils.

Our simulations suggest that the DNA is interwound by the histone at forces $f = 1.0$ and $2.0pN$, resulting in a relative extension $\bar{z}/L < 0.7$. The change in DNA extension due to nucleosome-wrapping, $\Delta z \equiv z_{nuc} - \bar{z}$ depends on the supercoiling (see FIG 5b). For the cases of $f = 1.0$ and $2.0pN$, $\Delta z^{(+)} < \Delta z^{(-)}$, leading to the work done being $-f\Delta z^{(+)} > -f\Delta z^{(-)}$. The smaller work done by force f results in reduced energy

bioRxiv preprint doi: https://doi.org/10.1101/2024.08.05.606726; this version posted August 6, 2024. The copyright holder for this preprint (which was not certified by peer review) is the author/funder. All rights reserved. No reuse allowed without permission.

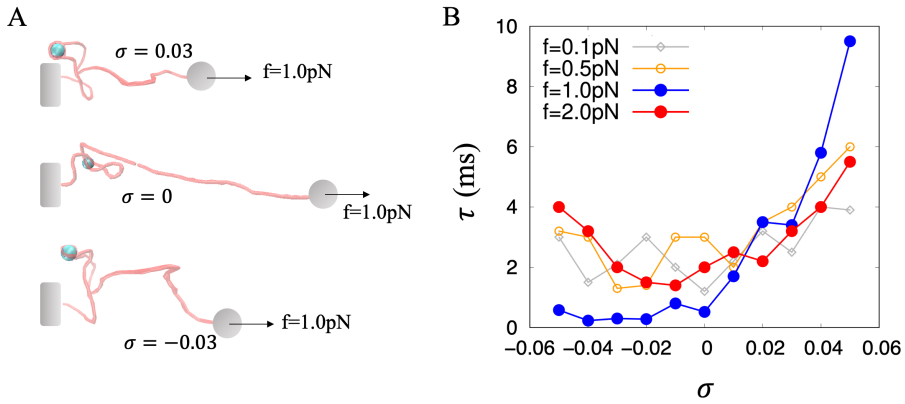


Fig 4. (A)Schematics for a single histone interacting with a supercoiled DNA under stretching force $f = 1.0pN$. (B) The supercoil-dependency of the MFPT for completing nucleosome wrapping. For the tensional DNA ($f \geq 0.5pN$), nucleosome wrapping prefers the negative supercoiled DNA.

barrier for nucleosome wrapping. Therefore, nucleosome wrapping tends to occur preferentially no negatively supercoiled DNA.

Discussion and Conclusion

For extendedly supercoiled DNA under $f = 0.1, 1.0$ or $2.0pN$, the induced $\Delta\Delta Lk = +1$ on the unconstrained DNA is primarily attributed to writhe, with $\Delta Wr \approx +1$ and $\Delta\Delta Tw \approx 0$ (FIG.6(a)). The increase in writhe rather than the change in twisting energy governs the dynamics. In other words, for positive writhe, $|Wr|$ increases due to nucleosome-wrapping. In contrast, for negative writhe, $|Wr|$ decreases due to nucleosome wrapping. Writhe measures the extent of DNA interwinding. Consequently, a significant magnitude of $|Wr|$ is associated with a reduced Δz. The negative supercoiling results in comparatively lower amount of work-done by f, implying a decreased energy barrier for nucleosome wrapping.

In FIG.6(a),we observed that as the force f increases, there is a corresponding increase in in $\Delta\Delta Tw$ and a decease in ΔWr. For highly tensional DNA, such as those subjected to $f = 5, 10$ and $20pN$, which are commonly utilized for stretching chromatin [12, 14], however, the increment of twist $\Delta\Delta Tw \approx 1$ meanwhile writhe $\Delta Wr \approx 0$ during nucleosome forming, giving a rise to a supercoiling-independent change in extension, $\Delta z = l_{nuc}$. The change of the twisting energy is supercoiling-dependent, i.e., $\Delta E_{\pm} = \frac{1}{2}C[(\Delta Lk \pm 1)^2 - (\Delta Lk)^2]$,where $C \equiv k_B T l_t (L - l_{nuc})\Omega_0^2/(Lk_0)^2$ is the stiffness of the whole unconstrained DNA [36]. Evidently, $\Delta E_+ > 0 > \Delta E_-$, meaning nucleosome-wrapping always prefers negative supercoils.

In both of the cases, the energy barrier associated with nucleosome wrapping under positively supercoiled DNA exceeds that of negatively supercoiled DNA, thereby the preference for negative supercoiling.

In eukaryotic chromatin, DNA attains a highly compact structure due to its wrapping around histone cores, contributing to negative supercoiling. To elucidate the mechanism underlying the spontaneous wrapping of supercoiled DNA around histone proteins, we designed a Brownian dynamics model of the DNA-histone complex. We demonstrated that both the positively and negatively supercoiled DNAs can form the nucleosome conformation at indiscriminate time scales with appropriate absorption energies between DNA and histone. Furthermore, we observed that the preference for

bioRxiv preprint doi: https://doi.org/10.1101/2024.08.05.606726; this version posted August 6, 2024. The copyright holder for this preprint (which was not certified by peer review) is the author/funder. All rights reserved. No reuse allowed without permission.

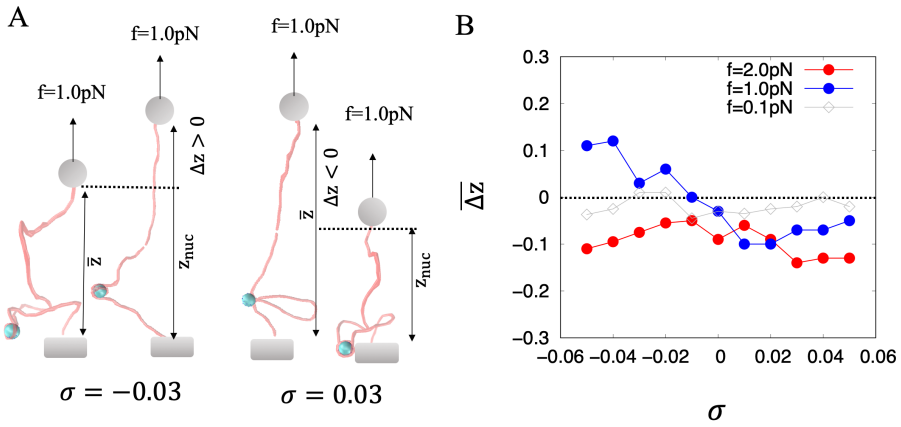


Fig 5. (A) The extension increment of the supercoiled DNA due to the nucleosome wrapping.Under $f = 1.0pN$, the nucleosome wrapping increases the extension of the negatively supercoiled DNA while reducing the extension of the positively supercoiled DNA. (B) The mean extension increment resulting from nucleosome wrapping is a function of supercoil density and stretching force. The positive increment in DNA extension due to nucleosome wrapping causes the decrease of the potential energy of the extended DNA, which is energetically favored.

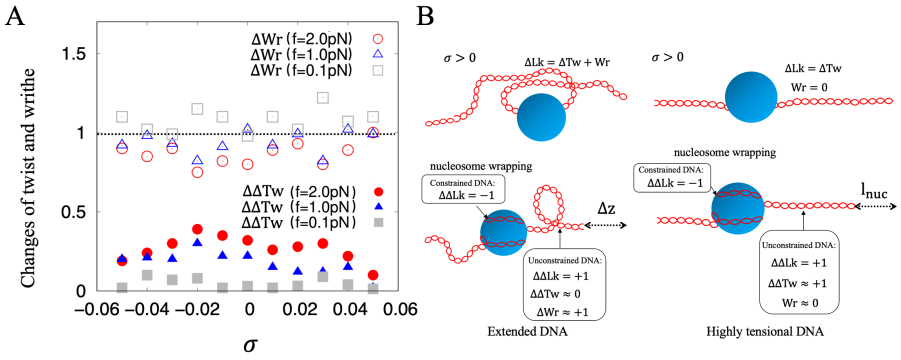


Fig 6. (A) Changes in the twist and writhe of the unconstrained DNA due to nucleosome-wrapping. (B)The changes in twist and writhe of (positive supercoils) DNA during winding around histone core. (Left) Extendedly (+) supercoiled DNA wraps around a histone under small force, e.g, $f = 0.5, 1.0$ and $2.0pN$. The induced +1 linking number is mainly attributed to writhe, which causes work done during nucleosome wrapping. (Right) Highly tensional (+) supercoiled DNA wraps around a histone under large force, e.g, $f = 10pN$. The induced +1 linking number is mainly attributed to twist, which increases twisting energy during nucleosome wrapping.

bioRxiv preprint doi: https://doi.org/10.1101/2024.08.05.606726; this version posted August 6, 2024. The copyright holder for this preprint (which was not certified by peer review) is the author/funder. All rights reserved. No reuse allowed without permission.

negative supercoiling during nucleosome wrapping becomes evident with increasing force. Several improvements to our model are warranted for future studies. The first one is the over-twist on the constrained DNA that wraps around histone, which may mainly originates from interaction with the histone rather than DNA intrinsic property [39]. Secondly, the nucleosome filament requires histone H1, which associates with the entry and exit of DNA from the histone core [21, 24]. The incorporation of the effects of the histone H1 allows nucleosomes to be arranged into a compact and stabilized array. In the large force regime, the dissociation of histone from DNA is dominating over re-assembling of nucleosome. Consequently, the net nucleosomes reassembling rate is determined by the difference between re-assembling rate and dissociate rate. Thus, the force-dependent kinetics of the nucleosome dissociation and re-assembling presents a promising research topic in the future.

Supporting information

S1 Text. Dynamics of the rotational degrees

S2 Text. Pathway of nucleosome wrapping and the intermediate states

acknowledgement

C.L. is supported by NSFC Grant #12005029 and start-up fund from Chongqing University of Posts and Telecommunication(A2020-029). B.W. is supported by NSFC Grant #12304246 and start-up fund from Wenzhou Institute, University of Chinese Academy of Sciences.

References

1. Bates AD, Maxwell A, Maxwell T, et al. DNA topology. Oxford University Press, USA; 2005.
2. Kornberg, Roger D. Structure of Chromatin. Annual Review of Biochemistry. 2003;46(1):931.
3. Arents G, Burlingame RW, Wang BC, Love WE, Moudrianakis EN. The nucleosomal core histone octamer at 3.1 A resolution: a tripartite protein assembly and a left-handed superhelix. Proceedings of the National Academy of Sciences. 1991;(22).
4. Luger K, Mader AW, Richmond RK, Sargent DF, Richmond TJ. Crystal structure of the nucleosome core particle at 2.8 A resolution. Nature. 1997;389(6648):251–260.
5. Song F, Chen P, Sun D, Wang M, Dong L, Liang D, et al. Cryo-EM Study of the Chromatin Fiber Reveals a Double Helix Twisted by Tetranucleosomal Units. Science. 2014;344(6182):376.
6. Hamkalo BA. Chromatin: Structure and function. Nato Advanced Study Institutes. 2006;9(4):7–14.
7. Kornberg RD, Lorch Y. Twenty-Five Years of the Nucleosome, Fundamental Particle of the Eukaryote Chromosome. 1999;.

bioRxiv preprint doi: https://doi.org/10.1101/2024.08.05.606726; this version posted August 6, 2024. The copyright holder for this preprint (which was not certified by peer review) is the author/funder. All rights reserved. No reuse allowed without permission.

8. Corless S, Gilbert N. Effects of DNA supercoiling on chromatin architecture. Biophysical reviews. 2016;8(3):245–258.

9. Kouzine F, Sanford S, Elisha-Feil Z, Levens D. The functional response of upstream DNA to dynamic supercoiling in vivo. Nature Structural & Molecular Biology. 2008;15(2):146.

10. Lavelle C. Pack, unpack, bend, twist, pull, push: the physical side of gene expression. Current opinion in genetics & development. 2014;25:74–84.

11. Allemand JF, Bensimon D, Croquette V. The elasticity of a single supercoiled DNA molecule (vol 271, pg 1835, 1996). Science. 1996;272(5263):797–797.

12. Cui Y, Bustamante C. Pulling a single chromatin fiber reveals the forces that maintain its higher-order structure. Proceedings of the National Academy of Sciences of the United States of America. 2000;97(1):p.127–132.

13. Le TT, Gao X, Park SH, Lee J, Wang MD. Synergistic Coordination of Chromatin Torsional Mechanics and Topoisomerase Activity. Biophysical Journal. 2020;118(3):374a.

14. Jaeyoon L, Meiling W, James T Inman ea. Chromatinization modulates topoisomerase II processivity. Nature Communications. 2023;14:6844.

15. Sakaue T, Yoshikawa K, Yoshimura SH, Takeyasu K. Histone Core Slips along DNA and Prefers Positioning at the Chain End. Physical Review Letters. 2001;87(7):78105–78105.

16. Mohammad-Rafiee F, Kuli IM, Schiessel H. Theory of Nucleosome Corkscrew Sliding in the Presence of Synthetic DNA Ligands. Journal of Molecular Biology. 2004;344(1):47–58.

17. Mochrie SGJ, Mack AH, Schlingman DJ, Collins R, Kamenetska M, Regan L. Unwinding and rewinding the nucleosome inner turn: Force dependence of the kinetic rate constants. Physical Review E. 2013;.

18. Stevens MJ, Kremer K. The nature of flexible linear polyelectrolytes in salt free solution: A molecular dynamics study. Journal of Chemical Physics. 1995;103(4):1669–1690.

19. Fujiwara S, Sato T. Molecular dynamics simulations of structural formation of a single polymer chain: Bond-orientational order and conformational defects. Journal of Chemical Physics. 1997;107(2):613.

20. Noguchi H, Yoshikawa K. Morphological variation in a collapsed single homopolymer chain. The Journal of Chemical Physics. 1998;109(12):5070–5077.

21. Mithun, Biswas, Karine, Voltz, Jeremy, C, et al. Role of Histone Tails in Structural Stability of the Nucleosome. PLoS Computational Biology. 2011;7(12):e1002279.

22. Hiroo K, Shoji T, Ilya I. Partial Unwrapping and Histone Tail Dynamics in Nucleosome Revealed by Coarse-Grained Molecular Simulations. PLOS Computational Biology. 2015;11(8):e1004443–.

23. Lequieu J, Cordoba A, Schwartz DC, De Pablo JJ. Tension-dependent Free Energies of Nucleosome Unwrapping. Acs Central Science. 2016;2(9):660.

bioRxiv preprint doi: https://doi.org/10.1101/2024.08.05.606726; this version posted August 6, 2024. The copyright holder for this preprint (which was not certified by peer review) is the author/funder. All rights reserved. No reuse allowed without permission.

24. Luque A, Ozer G, Schlick T. Correlation among DNA Linker Length, Linker Histone Concentration, and Histone Tails in Chromatin. Biophysical journal. 2016;110(11):2309–2319.

25. Parsons T, Zhang B. Critical role of histone tail entropy in nucleosome unwinding. The Journal of Chemical Physics. 2019;150(18):185103.

26. Noguchi H, Yoshikawa K. Folding path in a semiflexible homopolymer chain: A Brownian dynamics simulation. Journal of Chemical Physics. 2000;113(2):854–862.

27. Li W, Dou SX, Wang PY. Brownian Dynamics Simulation of Nucleosome Formation and Disruption under Stretching. Journal of Theoretical Biology. 2004;230(3):375–383.

28. Li W, Dou SX, Wang PY. The histone octamer influences the wrapping direction of DNA on it: Brownian dynamics simulation of the nucleosome chirality. Journal of Theoretical Biology. 2005;235(3):365–372.

29. Li W, Dou SX, Xie P, Wang PY. Brownian dynamics simulation of directional sliding of histone octamers caused by DNA bending. Phys Rev E Stat Nonlin Soft Matter Phys. 2006;73(5 Pt 1):051909.

30. Wocjan T, Klenin K, Langowski J. Brownian Dynamics Simulation of DNA Unrolling from the Nucleosome†. Journal of Physical Chemistry B. 2009;.

31. Higuchi Y, Sakaue T, Yoshikawa K. How does torsional rigidity affect the wrapping transition of a semiflexible chain around a spherical core? Physics. 2010;82(3):336–354.

32. Dobrovolskaia I, Arya G. Dynamics of Forced Nucleosome Unraveling and Role of Nonuniform Histone-DNA Interactions. Biophysical Journal. 2012;103(5):989–998.

33. Klenin K, Merlitz H, Langowski J. A Brownian dynamics program for the simulation of linear and circular DNA and other wormlike chain polyelectrolytes. Biophysical journal. 1998;74(2):780–788.

34. Vologodskii A. Brownian Dynamics Simulation of Knot Diffusion along a Stretched DNA Molecule. Biophysical Journal. 2006;90(5):1594–1597.

35. Ivenso ID, Lillian TD. Simulation of DNA supercoil relaxation. Biophysical journal. 2016;110(10):2176–2184.

36. Wan B, Yu J. Two-Phase Dynamics of DNA Supercoiling based on DNA Polymer Physics. Biophysical Journal. 2022;121(4):658–669.

37. Mielke SP, Fink WH, Krishnan VV, Grønbech-Jensen N, Benham CJ. Transcription-driven twin supercoiling of a DNA loop: a Brownian dynamics study. The Journal of chemical physics. 2004;121(16):8104–8112.

38. Al Masri C, Wan B, Yu J. Nonspecific vs. specific DNA binding free energetics of a transcription factor domain protein. Biophysical journal. 2023;122(22):4476—4487.

39. Hayes JJ, Bashkin J, Tullius TD, Wolffe AP. The histone core exerts a dominant constraint on the structure of DNA in a nucleosome. Biochemistry. 1991;30(34):8434.